Chemical Vapor Deposition Process on the ZSM-5(010) Surface as Investigated by Molecular Dynamics

Momoji Kubo, Yasunori Oumi, Hiromitsu Takaba, Abhijit Chatterjee, and Akira Miyamoto*

Department of Materials Chemistry, Graduate School of Engineering, Tohoku University,
Aoba-yama 07, Sendai 980-8579, Japan

The molecular dynamics (MD) method was applied to investigate a chemical vapor deposition process on the ZSM-5(010) surface. $Si(OH)_4$ molecules were placed on the ZSM-5(010) surface, and MD simulation was performed for 12 ps. We observed the formation and evaporation of H_2O molecules over the ZSM-5(010) surface. It indicates that the surface chemical reactions such as $Si(OH)_4$ + HO-[ZSM-5] → $Si(OH)_3$−O-[ZSM-5] + H_2O, $Si(OH)_3$−O-[ZSM-5] + $Si(OH)_3$−O-[ZSM-5] → [ZSM-5]-O−$Si(OH)_2$−O−$Si(OH)_2$−O-[ZSM-5] + H_2O and others, take place during the MD simulation. The formation of new Si−O−Si bonds was also observed on the surface, indicating the crystal growth of the ZSM-5(010) surface. Moreover, the constructed SiO_2 layer was not amorphous, but inherited the ZSM-5 structure, keeping the 10-membered ring and (010) oriented configuration. Hence, we confirmed that the MD method was effective for reproducing and investigating the chemical vapor deposition process on zeolite surfaces on an atomic scale.

1. Introduction

Zeolites have been widely applied to catalysts, adsorbents, molecular sieves, builders, building materials, and so on. A discovery of novel zeolite framework structure has given great impacts on industry, engineering, and science. Especially the development of Y-type zeolite enabled us to industrialize the catalytic cracking process, while the development of ZSM-5 zeolite enabled us to industrialize the methanol to gasoline (MTG) process, isomerization of xylene, and many other processes. Recently, the discovery of mesoporous materials such as MCM-41 and FSM-16 gained much attention because their large pore size enables us to realize the catalytic reactions of larger organic molecules that have not been achieved in the small micropore of zeolites. Although a lot of studies on the effects of zeolite structures, exchanged cations, and framework cations on the catalytic activity and selectivity have been carried out, a significantly lower number of researches on the development of novel zeolite framework structure has been performed despite their intense demand, because of its difficulties and long time consumption. Hence, a new efficient technology on the design and development of a novel zeolite framework structure is greatly required instead of traditional trial and error experiments.

On the other hand, recently theoretical approaches such as molecular dynamics (MD), quantum chemistry (QC), and Monte Carlo simulation (MC) gained much attention in the zeolite chemistry. Recent advances and developments of computational chemistry on zeolites have been reported in some exhaustive reviews,[1−6] and we have also reported a lot of applications of MD, QC, and MC methods to zeolites and related microporous materials.[7−9] Owing to its great advances and developments, the computational chemistry is also expected to play an important role for the design and development of novel zeolite framework structure. However, computational chemistry has been traditionally applied to a catalytic mechanism, activity, selectivity, stability, and structure of zeolites as well as diffusion and adsorption of molecules inside zeolite pores, and a few simulation studies were devoted to the synthesis process of zeolites because of its difficulties and the lack of appropriate force fields to reproduce the crystal growth processes.

More recently, Catlow et al. applied[10] the molecular mechanics method to the design of organic template molecules for zeolite synthesis. To the best of our knowledge, it is a first simulation algorithm related to the zeolite synthesis. However, it does not enable us to design novel zeolite framework structures. On the other hand, recently, we developed[11] a crystal growth MD simulator and applied it to the homoepitaxial growth process of MgO(001),[11] $SrTiO_3$(001),[12,13] and ZnO(0001)[14] surfaces as well as the heteroepitaxial growth process of ultrafine Au particles on the MgO(001) surface[15,16] and BaO layers on the $SrTiO_3$(001) surface.[17] In the above crystal growth MD simulations, metal oxide molecules or metal atoms are continuously deposited on the substrates and the deposited molecules or atoms stack on the substrate without surface chemical reactions. However, the above simulation methodology for the crystal growth process is not sufficient for the simulation of the zeolite synthesis process, since the surface of zeolites is normally terminated by the silanol groups (HO-[zeolite]) and the simulations on the surface chemical reaction processes such as $Si(OH)_4$ + HO-[zeolite] → $Si(OH)_3$−O-[zeolite] + H_2O are required. The treatment of the above surface chemical reactions is crucial for the classical MD simulations and has prohibited simulation of the synthesis process of zeolites. However, we thought that the construction of appropriate force fields for the above surface chemical reactions on zeolite surfaces and the development of a new MD algorithm for the simulation of the zeolite synthesis processes enable us to simulate the crystal growth process of zeolites.

Hence, in the present study we determined the novel force field, which can reproduce the surface chemical reactions on zeolites, and applied our MD simulation code to the chemical
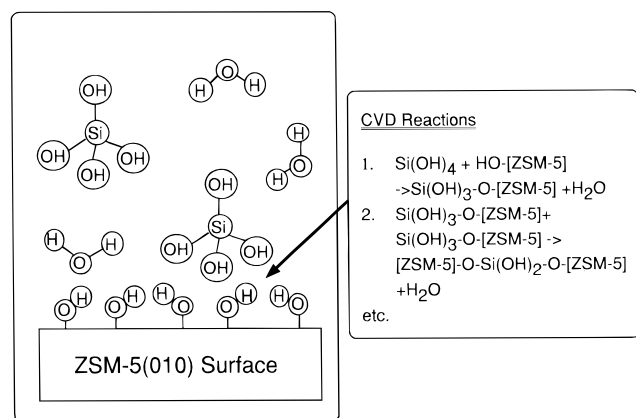
Chemical Vapor Deposition Process on the ZSM-5(010)

J. Phys. Chem. B, Vol. 103, No. 11, 1999 **1877**

Figure 1. Employed model system for the MD simulation of CVD process on ZSM-5(010).

vapor deposition (CVD) process on the ZSM-5(010) surface as a first step of the MD simulation on the zeolite synthesis process.

2. Method

We employed our MD simulation code MOMODY Ver. 1.0. The Verlet algorithm was used for the calculation of atomic motions, while the Ewald method was applied for the calculation of electrostatic interactions. Temperature was controlled by means of scaling the atom velocities under periodic boundary conditions. The calculations were performed for 30 000 steps with a time step of 0.4×10^{-15} s. To simplify the model, we employed $Si(OH)_4$ molecules as a CVD source. Figure 1 shows a model system for the MD simulation of the CVD process, and totally 12 $Si(OH)_4$ molecules were placed on the ZSM-5(010) surface. In the present MD unit cell, the ZSM-5(010) surface is terminated by eight silanol groups. The interatomic potential functions consist of two-body and three-body terms. The two-body, central force, interatomic potential is described as follows for any atom pairs. In eq 1, the first, second, and third terms refer to Coulomb, exchange repulsion, and Morse interactions, respectively.

$$u(r_{ij}) = Z_i Z_j e^2 / r_{ij} + f_o(b_i + b_j) \exp[(a_i + a_j - r_{ij})/(b_i + b_j)] \\ + D_{ij}[\exp\{-2\beta_{ij}(r_{ij} - r_{ij}^*)\} - 2\exp\{-\beta_{ij}(r_{ij} - r_{ij}^*)\}] \quad (1)$$

where Z_i is the atomic charge, e is the elementary electric charge, r_{ij} is the interatomic distance, and f_o is a constant for unit adaptations. The parameters a and b represent the size and stiffness, respectively, in the exchange repulsion interaction, while D_{ij}, r_{ij}^*, and β_{ij} represent bond energy, equilibrium bond distance, and stiffness, respectively, in the Morse function. The equations for three-body potential are described and discussed in the following section. Moreover, dynamic features in the CVD process were investigated by using computer graphics visualization with the MOMOVIE and RYUGA[18] codes developed in our laboratory on an OMRON LUNA88K workstation and a Hewlett-Packard Model 715/33 workstation, respectively.

3. Results and Discussion

A lot of accurate force fields for silica and zeolite systems[19−29] were constructed by using QC and MD calculations, and many interesting MD simulations on silica and zeolite systems have been carried out by using the above force fields. Some of them employ three-body potentials related to Si−O−Si or O−Si−O bond angles, in addition to two-body potentials including

Figure 2. Comparison of H_2O, $Si(OH)_4$, and ZSM-5 structures obtained by the present MD simulataions, ab initio calculations and experiment.

TABLE 1: Potential Parameters for Si, O, and H Atoms

atom	Z_i	a_i/Å	b_i/Å	c/Å^3 (kJ/mol)$^{1/2}$
O	−0.8	1.814	0.150	83.7
Si	+1.6	0.703	0.100	0.0
H	+0.4	0.058	0.060	0.0

atom pairs	D_{ij}/kJ mol^{-1}	β_{ij}/Å^{-1}	r_{ij}^*/Å
O−Si	125.5	2.00	1.51
O−H	146.4	2.74	0.96

3-body	f_k/10^{-19} J	θ_0/deg	r_{m1}/Å	r_{m2}/Å	g_{r1}/Å^{-1} & g_{r2}/Å^{-1}
O−Si−O	2.2	109.5	1.90	1.90	7.0
Si−O−Si	0.7	158.0	1.90	1.90	7.0
Si−O−H	0.9	109.5	1.90	1.40	7.0
H−O−H	1.5	95.0	1.40	1.40	7.0

Coulomb, exchange repulsion, and bond terms. However, normally those three-body potentials are functions of only three-body angles but not of two-body distances, and the information on atomic connectivities is essential to applying the three-body potentials. Even if the Si−O distance increases much longer than the regular Si−O bond distance (1.5−1.6 Å) due to the bond dissociation, the Si−O−Si or O−Si−O angle terms work as if they still connect with each other because the initial information on the atomic connectivities are not modified during the MD simulations. Similarly, even if two $Si(OH)_4$ molecules approach each other from infinity, the Si−O−Si angle term does not work because the initial information on the atomic connectivities does not include the Si−O−Si bond in the two $Si(OH)_4$ molecules. Hence, the processes including the dissociation and formation of Si−O bonds cannot be simulated by using such three-body potential functions.

Recently, Galofalini et al.[30] developed a novel force field including three-body potential for amorphous silica systems, which allows the dissociation and formation of Si−O and O−H bonds. They successfully applied it to the simulation of the crystal growth process of amorphous silica systems.[30,31] However, they have not applied it to the crystal growth process of zeolites. On the other hand, recently Kawamura et al. reported[32] the development of novel three-body potential functions for H_2O molecules, which allows the dissociation and formation of O−H bonds. Especially, they confirmed that their potential function well reproduces the formation of hydrogen bonds in H_2O liquid. Hence, we expanded their three-body potential equations in order to apply them to zeolite systems. The expanded three-body potentials, which are a function not only of three-body angles but also of two-body distances, enable us to simulate the formation and dissociation of Si−O and O−H bonds. Since the information on the atomic connectivities in ZSM-5 is not
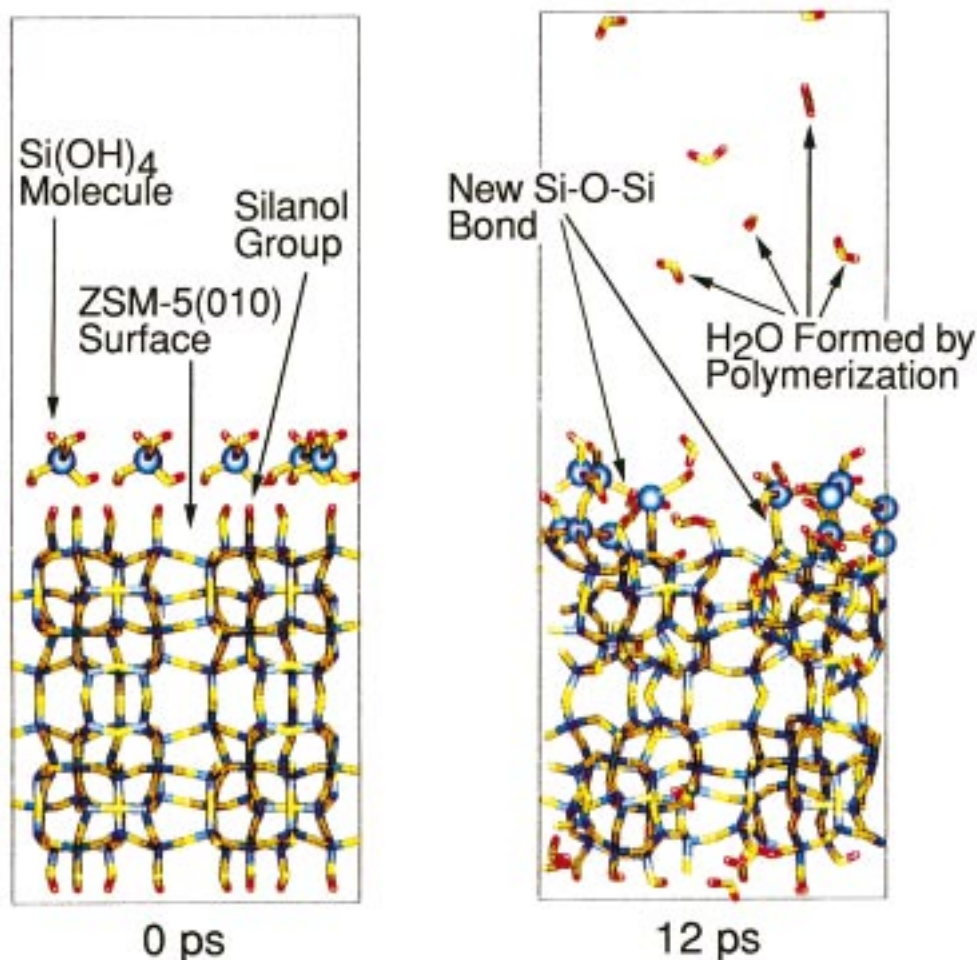
Figure 3. Chemical vapor deposition process of $Si(OH)_4$ molecules on the ZSM-5(010) surface.

required for the expanded potential function, the chemical reactions on the ZSM-5 surface can be simulated.

The three-body potential, as shown in eq 2, is applied for Si−O−H, Si−O−Si, O−Si−O, and H−O−H angles.

$$u(\theta_{ijk}) = -f_k[\cos\{2(\theta_{ijk} - \theta_o)\} - 1] (k_1 k_2)^{1/2} \qquad (2)$$

where θ_{ijk} is the i−j−k angle and f_k and θ_o are the parameters. The variables k_1 and k_2 define the effective range of the three-body potential:

$$k_1 = 1/[\exp\{g_{r1}(r_{ij} - r_{m1})\} + 1] \qquad (3)$$

$$k_2 = 1/[\exp\{g_{r2}(r_{jk} - r_{m2})\} + 1] \qquad (4)$$

where g_{r1}, g_{r2}, r_{m1}, and r_{m2} are the parameters. r_{ij} and r_{jk} are i−j and j−k distances, respectively. The values of k_1 and k_2 are about unity at the regular bond distance of two atoms and approach zero with the increment of the distance. The potential parameters for zeolite systems were determined (Table 1) by verifying the reproduction of H_2O, $Si(OH)_4$, and ZSM-5[33−35] structures (Figure 2).

The CVD simulation was performed at a high temperature of 1500 K, according to the previous work on the formation of a silica−alumina interface by Garofalini et al.[36] It allows for observation of the reaction kinetics during a time accessible in MD simulations. Although the simulation temperature may seem to be slightly high, it is only about 40% of the simulated melting temperature of ZSM-5 with the present potentials. Figure 3 shows the CVD process of $Si(OH)_4$ molecules on the ZSM-
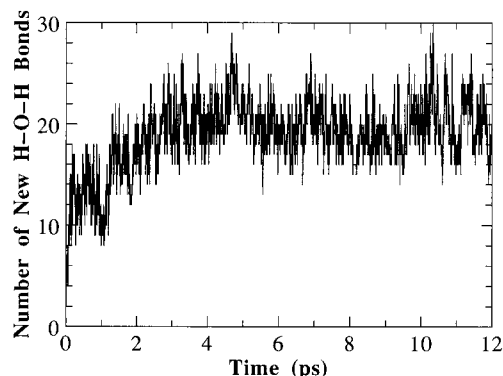

Figure 4. Change in the number of H_2O molecules during the CVD process on the ZSM-5(010) surface.

5(010) surface at 1500 K. The ZSM-5(010) substrate is shown by atomic bonds, while the Si atoms of the deposited $Si(OH)_4$ molecules are shown by spheres and other atoms of the $Si(OH)_4$ molecules are shown by atomic bonds. The formation and evaporation of H_2O molecules over the ZSM-5(010) surface was observed. It indicates that the surface chemical reactions such as (5) $Si(OH)_4$ + HO-[ZSM-5] → $Si(OH)_3$−O-[ZSM-5], (6) $Si(OH)_3$−O-[ZSM-5] + $Si(OH)_3$−O-[ZSM-5] → [ZSM-5]-O−$Si(OH)_2$−O−$Si(OH)_2$−O-[ZSM-5] and others take place during the CVD process simulation. Figure 4 shows the change in the number of H_2O molecules as a function of time during the CVD process on the ZSM-5(010) surface. No H_2O molecules existed at 0 ps and the rapid formation of H_2O molecules was observed. The number of SiOH species in the system was
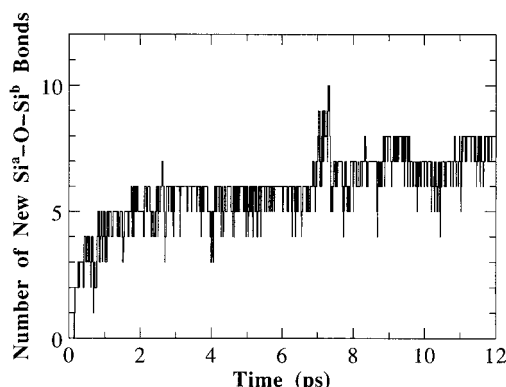
Chemical Vapor Deposition Process on the ZSM-5(010)

J. Phys. Chem. B, Vol. 103, No. 11, 1999 **1879**

Figure 5. Change in the number of new Si^a–O–Si^b bonds during the CVD process on the ZSM-5(010) surface. Si^a: Si of $Si(OH)_4$ molecules. Si^b: Si of silanol groups of the ZSM-5(010) surface.

Figure 6. Change in the number of new Si^a–O–Si^a bonds during the CVD process on the ZSM-5(010) surface. Si^a: Si of $Si(OH)_4$ molecules.

reduced with time, and hence the formation of H_2O molecules was saturated after 4 ps and finally 20 H_2O molecules were formed.

Attention was given to the Si atoms represented by spheres on the ZSM-5(010) surface at 12 ps (Figure 3), which originally come from the $Si(OH)_4$ molecules. All the above Si atoms connected to the ZSM-5(010) surface or other $Si(OH)_4$ molecules, indicating the formation of new Si–O–Si bonds. It shows that the surface chemical reactions, eqs 5 and 6, take place on the ZSM-5(010) surface. Hence, we confirmed that the crystal growth process including the surface chemical reactions can be reproduced by the MD simulations and empirical force field. Moreover, the constructed SiO_2 layer was not amorphous but inherited the ZSM-5 structure, keeping the 10-membered ring and (010) oriented configuration. These results indicate that the epitaxial growth of ZSM-5(010) is realized in the CVD crystal growth simulation. Figure 5 shows the change in the number of Si^a–O–Si^b bonds during the CVD process on the ZSM-5(010) surface (Si^a, Si of $Si(OH)_4$ molecules; Si^b, Si of silanol groups of the ZSM-5(010) surface). After the rapid formation of six Si^a–O–Si^b bonds was observed during the first 2 ps, the formation of Si^a–O–Si^b bonds was gradually saturated and finally eight Si^a–O–Si^b bonds were formed in the system. It indicates that the surface chemical reaction, eq 5, takes place on the surface. The eight $Si(OH)_4$ molecules among all twelve deposited $Si(OH)_4$ molecules directly connected to the eight silanol groups of the ZSM-5(010) surface. Since totally eight silanol groups exist at the initial stage of the MD simulation, whole silanol groups of the ZSM-5(010) surface were found to react with the deposited $Si(OH)_4$ molecules. It indicates that the ideal one coordination between the $Si(OH)_4$ molecule and silanol group was realized at all silanol group positions. It is also a proof for the realization of the epitaxial growth of the ZSM-5(010) surface.

Figure 6 shows the change in the number of new Si^a–O–Si^a bonds during the CVD process on the ZSM-5(010) surface (Si^a: Si of $Si(OH)_4$ molecules). The number of Si^a–O–Si^a bonds increased rapidly with time during the first 4 ps. The formation of Si^a–O–Si^a bonds was gradually saturated, and finally, twelve Si^a–O–Si^a bonds were detected in the system. It indicates that the surface chemical reactions, eqs 5 and 6, take place on the surface. The formation of Si^a–O–Si^b bonds shows the formation of Si–O bond networks horizontal to the ZSM-5(010) surface, while that of Si^a–O–Si^a bonds shows the formation of Si–O bond networks perpendicular to the ZSM-5(010) surface. Hence, we confirmed that the formation of both perpendicular and horizontal Si–O–Si bond networks can be simulated by the MD method and empirical force field.
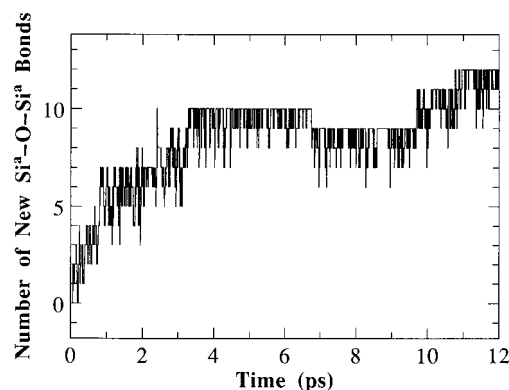
4. Conclusion

We successfully simulated the CVD process of $Si(OH)_4$ molecules on the ZSM-5(010) surface by using the MD technique. It is greatly due to the construction of a new force field, which allows the dissociation and formation of O–H and Si–O bonds and which can simulate the surface chemical reactions on the ZSM-5(010) surface. We hope that the crystal growth MD simulations of zeolites will have a important role in the design of novel zeolite framework structures. Especially the incorporation of organic templates and solvents in the crystal growth MD simulations of zeolites will be realized in the near future, and those crystal growth MD simulations will have a great impact on the zeolite chemistries and industries.

References and Notes

(1) Sauer, J. *Chem. Rev.* **1989**, *89*, 199.
(2) Catlow, C. R. A.; Cox, P. A.; Jackson, R. A.; Parker, S. C.; Price, G. D.; Tomlinson, S. M.; Vetrivel, R. *Mol. Simul.* **1989**, *3*, 49.
(3) Catlow, C. R. A., Ed. *Modeling of Structure and Reactivity in Zeolites*; Academic Press: London, 1992.
(4) Sauer, J.; Ugliengo, P.; Garrone, E.; Saunders, V. R. *Chem. Rev.* **1994**, *94*, 2095.
(5) Miyamoto, A., Hattori, T., Misono, M., Eds. *The Impact of Computers on Catalyst Research and Development*; Elsevier: Amsterdam, 1995.
(6) van Santen, R. A.; Kramer, G. J. *Chem. Rev.* **1995**, *95*, 637.
(7) Broclawik, E.; Himei, H.; Yamadaya, M.; Kubo, M.; Miyamoto, A.; Vetrivel, R. *J. Chem. Phys.* **1995**, *103*, 2102.
(8) Mizukami, K.; Takaba, H.; Oumi, Y.; Katagiri, M.; Kubo, M.; Stirling, A.; Broclawik, E.; Miyamoto, A. *Stud. Surf. Sci. Catal.* **1997**, *105*, 1811.
(9) Takaba, H.; Koshita, R.; Mizukami, K.; Oumi, Y.; Ito, N.; Kubo, M.; Fahmi, A.; Miyamoto A. *J. Membr. Sci.* **1997**, *134*, 127.
(10) Lewis, D. W.; Willock, D. J.; Catlow, C. R. A.; Thomas, J. M.; Hutchings, G. J. *Nature* **1996**, *382*, 604.
(11) Kubo, M.; Oumi, Y.; Miura, R.; Fahmi, A.; Stirling, A.; Miyamoto, A.; Kawasaki, M.; Yoshimoto, M.; Koinuma, H. *J. Chem. Phys.* **1997**, *107*, 4416.
(12) Kubo, M., Oumi, Y.; Miura, R.; Stirling, A.; Miyamoto, A.; Kawasaki, M.; Yoshimoto, M.; Koinuma, H. *Phys. Rev. B* **1997**, *56*, 13535.
(13) Kubo, M.; Oumi, Y.; Miura, R.; Stirling, A.; Miyamoto, A.; Kawasaki, M.; Yoshimoto, M.; Koinuma, H. *J. Chem. Phys.* **1998**, *109*, 8601.
(14) Kubo, M.; Oumi, Y.; Takaba, H.; Teraishi, K.; Chatterjee, A.; Miyamoto A. *Phys. Rev. B*, under contibution.
(15) Kubo, M.; Yamauchi, R.; Vetrivel, R.; Miyamoto, A. *Appl. Surf. Sci.* **1994**, *82/83*, 559.
(16) Kubo, M.; Miura, R.; Yamauchi, R.; Vetrivel, R.; Miyamoto, A. *Appl. Surf. Sci.* **1995**, *89*, 131.
(17) Kubo, M.; Oumi, Y.; Miura, R.; Stirling, A.; Miyamoto, A.; Kawasaki, M.; Yoshimoto, M.; Koinuma, H. *J. Chem. Phys.* **1998**, *109*, 9148.
(18) Miura, R.; Yamano, H.; Yamauchi, R.; Katagiri, M.; Kubo, M.; Vetrivel, R.; Miyamoto, A. *Catal. Today* **1995**, *23*, 409.

(19) Sander, M. J.; Leslie, M.; Catlow, C. R. A. *J. Chem. Soc., Chem. Commun.* **1984**, 1271.

(20) Tsuneyuki, S.; Tsukada, M.; Aoki, H.; Matsui, Y. *Phys. Rev. Lett.* **1988**, *61*, 869.

(21) Maya, S. L.; Olafson, B. D.; Goddard, W. A., III. *J. Phys. Chem.* **1990**, *94*, 8897.

(22) van Beest, B. W. H.; Kramer, G. J.; van Santen, R. A. *Phys. Rev. Lett.* **1990**, *64*, 1955.

(23) Kramer, G. J., Farragher, N. P.; van Beest, B. W. H.; van Santen, R. A. *Phys. Rev. B* **1991**, 43, 5068.

(24) de Vos Burchart, E.; Verheij, V. A.; van Bekkum, H.; van de Graaf, B. *Zeolites* **1992**, *12*, 183.

(25) Rappe, A. K.; Casewit, C. J.; Colwell, K. S.; Goddard, W. A., III; Skiff, W. M. *J. Am. Chem. Soc.* **1992**, *114*, 10024.

(26) Kawamura, K. *Solid-State Sci.* **1992**, *103*, 88.

(27) Hill J.-R.; Sauer, J. *J. Phys. Chem.* **1994**, *98*, 1238.

(28) de Boer, K.; Jansen, A. P. J.; van Santen, R. A. *Chem. Phys. Lett.* **1994**, *223*, 46.

(29) Yamahara, K.; Okazaki, K.; Kawamura, K. *Catal. Today* **1995**, *23*, 397.

(30) Feuston, B. P.; Garofalini, S. H. *J. Phys. Chem.* **1990**, *94*, 5351.

(31) Garofalini, S. H.; Martin, G. *J. Phys. Chem.* **1994**, *98*, 1311.

(32) Kumagai, N.; Kawamura, K.; Yokokawa, T. *Mol. Simul.* **1994**, *12*, 177.

(33) Simandiras, E. D.; Amos, R. D.; Handy, N. C. *Chem. Phys.* **1987**, *114*, 9.

(34) Gibbs, G. V.; D'Arco, P.; Boisen, M. B., Jr. *J. Phys. Chem.* **1987**, *91*, 5347.

(35) Olson, D. H.; Kokotailo, G. T.; Lawton, S. L.; Meier, W. M. *J. Phys. Chem.* **1981**, *85*, 2238.

(36) Blonsli, S.; Garofalini, S. H. *J. Phys. Chem.* **1996**, *100*, 2201.